



Influence of isothermal and cyclic annealing on structure and swelling of neutron-irradiated beryllium

D.V. Andreev ^{*}, V.N. Bespalov, A.Yu. Biryukov, E.A. Krasikov

Russian Research Center, Kurchatov Institute, Kurchatov square 1, 123182 Moscow, Russian Federation

Received 16 November 1998; accepted 8 March 1999

Abstract

The influence of cyclic and isothermal annealing on structure and swelling of neutron-irradiated beryllium was examined. At cyclic annealing the base temperature was equal to 150°C, the maximum cycle temperature was 600°C (700°C in the second experimental set), the number of heating-cooling cycles was from 10 to 100. Isothermal annealing of beryllium was performed at 600°C, 700°C and 800°C. The annealing time in the isothermal regime was the same as well as the total annealing time of beryllium samples at appropriate temperatures in the cyclic regime. It was shown that there are no significant differences in the influence of cyclic and isothermal annealing on structure and swelling of irradiated beryllium. © 1999 Elsevier Science B.V. All rights reserved.

PACS: 28.52.Fa; 28.52.Nh; 28.41.T

1. Introduction

In accordance with the ITER concept, the first wall and the limiter will be shielded by a beryllium armor of about 10 mm thickness [1,2]. It is assumed that the beryllium temperature in this application will be varied from 160°C to 587°C and a neutron fluence will achieve values of about $3 \times 10^{21} \text{ cm}^{-2}$ after the basic performance phase (BPP, 6000 cycles) and about $8 \times 10^{21} \text{ cm}^{-2}$ after the enhanced performance phase (EPP, 32 000 cycles) [1–3]. So, beryllium armor plates will work under high thermal cycling and neutron irradiation conditions.

Previous investigations of neutron-irradiated beryllium were performed usually in steady-state heating regimes. There are some works dedicated to the examination of beryllium under annealing at temperature changes in some range. For example, in Ref. [4] the swelling of neutron-irradiated beryllium was higher after cyclic annealing in comparison with isothermal annealing at the same temperature. In Ref. [5] it was shown that the swelling under the stepwise isochronal annealing

at rising temperatures was smaller than that for the once-annealed samples. The direct thermal cycling of the beryllium–copper water-cooled plate under these electron beam heating shows the visible crack formation [6,7].

This paper presents the results of the influence of cyclic and isothermal annealing on structure and swelling of neutron-irradiated beryllium (Russian hot-pressed beryllium TShG-200 type, see Table 1).

2. Materials and experimental techniques

The samples were cut from a hot-pressed beryllium rod irradiated at 100°C in the MR reactor [5,8]. Fast neutron fluences for these samples were 1×10^{21} , 3×10^{21} , $9 \times 10^{21} \text{ cm}^{-2}$ ($E > 0.5 \text{ MeV}$). The prismatic shape samples for the annealing were cut by the electro-sparg technique. The sample sizes were $3 \times 3 \times 3 \text{ mm}^3$ for a neutron fluence of $1 \times 10^{21} \text{ cm}^{-2}$, $3 \times 4 \times 5 \text{ mm}^3$ for neutron fluences of 3×10^{21} and $9 \times 10^{21} \text{ cm}^{-2}$. For comparison unirradiated beryllium samples with the size $3 \times 4 \times 5 \text{ mm}^3$ were also prepared. Before annealing the density of the samples was determined by hydrostatic weighing (see Table 1).

^{*} Corresponding author. Tel.: +7-095 1969528; fax: +7-095 1961701; e-mail: andreev@nw.oirtorm.net.kiae.su

Table 1
Investigated beryllium data

Fluence (cm ⁻²)	Impurities content (wt%)			Transmutation gases content (appm)		Beryllium density, (g cm ⁻³)
	O	C	Fe	³ H	⁴ He	
0	0.8	0.1	0.07	0	0	1.845
1 × 10 ²¹	0.8	0.1	0.07	Not measured	Not measured	1.839
3 × 10 ²¹	0.8	0.1	0.07	370 ± 70	1880 ± 360	1.837
9 × 10 ²¹	0.8	0.1	0.07	785 ± 155	4400 ± 400	1.816

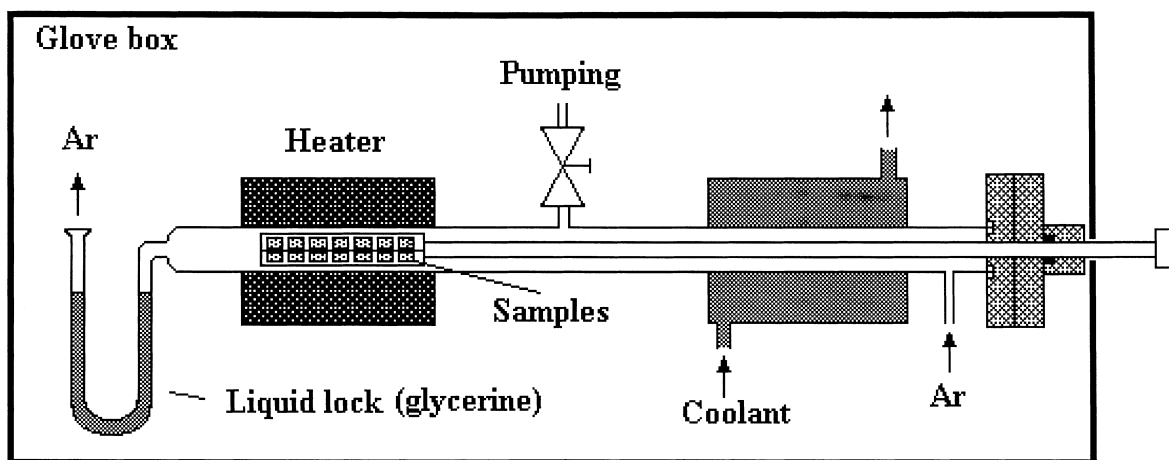


Fig. 1. Experimental installation.

For the experiments a silica tube furnished by the external heater zone and water cooled zone was used, a sample holder was moved from one zone to the other by a rod that was introduced into the tube through a vacuum tight Wilson collar (Fig. 1). Before the experiment the tube volume was evacuated to a pressure lower than 10 Pa and after that the tube volume was purged continuously by argon at an exceeding pressure about 1 kPa and a flow rate about 100 cm³ min⁻¹. The sample temperature was registered by the thermocouple attached to the sample holder.

There were two basic cyclic annealing regimes:

1. Heating of all samples listed in Table 1 up to a temperature of 600°C or 700°C (about 100–150 s), exposure of the samples at this temperature (about 850–900 s), cooling down to 150°C (about 150 s), etc.
2. Heating of the samples irradiated with a neutron fluence of 9×10^{21} cm⁻² ($E > 0.5$ MeV) up to a temperature of 700°C (about 80 s), cooling down to 150°C (about 150 s), etc.

The temperature choice was determined by the circumstance that the temperature 600°C was an ITER project data [1,2,7] and 700°C was the margin condition to be checked. The number of cycles in the first regime mentioned above was 10°C, 30°C and 100°C for 600°C

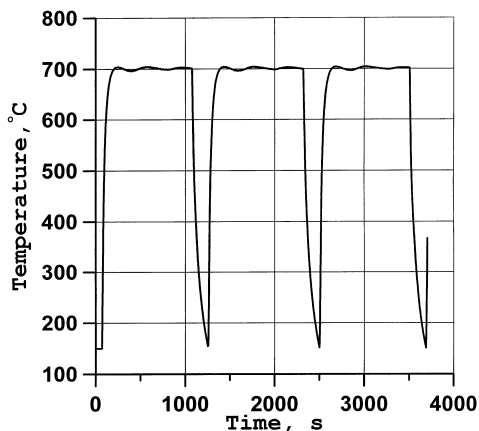


Fig. 2. Typical temperature change curve during cyclic annealing with sample exposure at the maximum cycle temperature.

and 10°C, 30°C and 110°C for 700°C. The typical temperature change curve in these cases is presented in Fig. 2. Moreover, the isothermal annealings were conducted at 600°C, 700°C and 800°C of the same performance samples. The annealing time in the isothermal

regime was the same as well as the total annealing time of beryllium samples at the appropriate temperature in the cyclic regime. Namely, the isothermal annealing time at 600°C was 86 700 s (corresponding to 100 cycles) and at 700°C it was 26 300 and 94 600 s (corresponding to 30 and 110 cycles, respectively).

The beryllium samples irradiated with a neutron fluence of $9 \times 10^{21} \text{ cm}^{-2}$ ($E > 0.5 \text{ MeV}$) were used for the cyclic annealing in accordance with the second regime. The number of cycles was 10, 30, 60 and 100. The typical temperature change curve in this case is presented in Fig. 3. Two samples with the same fluence were annealed in a specially fitted quasi-steady-state regime with the smooth temperature rising (see Fig. 4) to clear up the cyclic annealing effect. The quasi-steady-state annealing regime was determined from equation $\tau(\Delta T) = \sum_{n=1}^N \tau_n(\Delta T)$, i.e. in the quasi-steady-state

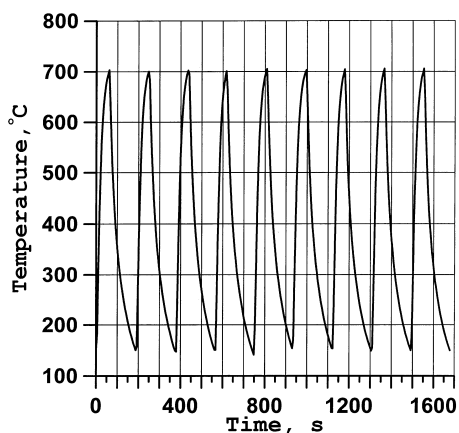


Fig. 3. Typical temperature change curve during cyclic annealing without sample exposure at the maximum cycle temperature.

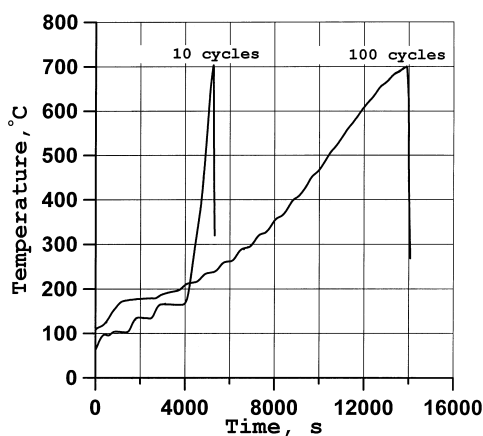


Fig. 4. Temperature change curves during annealing in the quasi-steady-state regime.

regime, the exposure $\tau(\Delta T)$ of the sample in the each temperature region ΔT was equal to the total exposure in the same region ΔT after N cycles. The comparison with 10 and 100 cycles was performed. After annealing the sample density was determined by hydrostatic weighing. For the optical microscopy examination the samples were impregnated under vacuum by an epoxy resin.

3. Experimental results

Fig. 5 presents the neutron-irradiated beryllium swelling dependence on the duration of the cyclic or isothermal annealing at 600°C. The swelling of the beryllium samples with a neutron fluence of $3 \times 10^{21} \text{ cm}^{-2}$ after the cyclic (100 cycles) and isothermal (86 700 s) annealing was $0.7 \pm 0.3\%$ and $0.6 \pm 0.3\%$, correspondingly. At the same time the swelling of the beryllium samples with a neutron fluence of $9 \times 10^{21} \text{ cm}^{-2}$ was equal to $2.3 \pm 0.4\%$ in both cases. For the samples with a neutron fluence of $1 \times 10^{21} \text{ cm}^{-2}$ the swelling dependence from the annealing duration was very close to the same for the samples with a neutron fluence of $3 \times 10^{21} \text{ cm}^{-2}$.

Fig. 6 presents the neutron beryllium swelling dependence on the duration of the cyclic or isothermal annealing at 700°C. The noticeable swelling of the samples irradiated with a neutron fluence of $9 \times 10^{21} \text{ cm}^{-2}$ occurred after 10 cycles. After 30 cycles it achieved a value of $14.5 \pm 0.4\%$. The swelling of the sample with the same neutron fluence after the corresponding isothermal annealing at 700°C was very close to this value. The swelling of the samples with a neutron fluence of $3 \times 10^{21} \text{ cm}^{-2}$ was also significantly higher than that

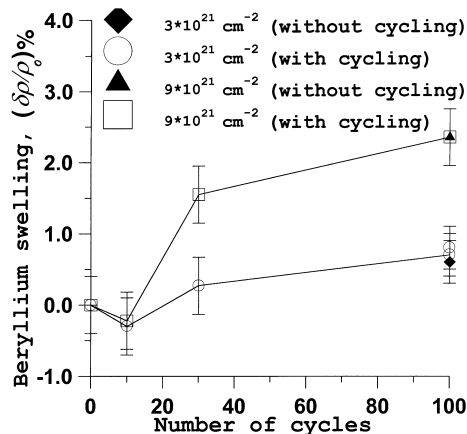


Fig. 5. Neutron-irradiated beryllium swelling dependence on the annealing duration in cyclic (with exposure at maximum cycle temperature) and isothermal regimes (maximum cycle temperature of 600°C). ρ_0 – beryllium density before annealing.

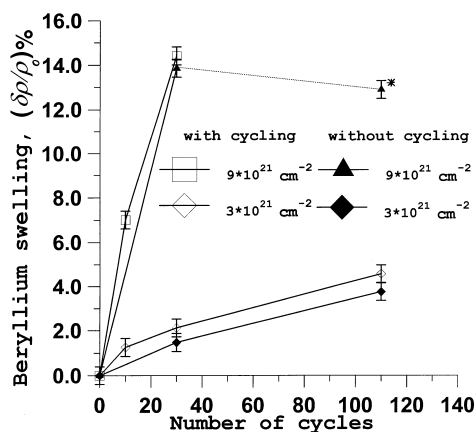


Fig. 6. Neutron-irradiated beryllium swelling dependence on the annealing duration in cyclic (with exposure at maximum cycle temperature) and isothermal regimes (maximum cycle temperature of 700°C). ρ_0 – beryllium density before annealing, (*) – result for the crashed sample fragment (see details in the text).

after annealing at 600°C. After 110 cycles it achieved a value about 4%. The density change of the samples irradiated with this fluence and isothermally annealed at 700°C was slightly lower.

It was observed that the beryllium samples irradiated with a neutron fluence of $9 \times 10^{21} \text{ cm}^{-2}$ were destroyed after 110 cycles of annealing at 700°C, the same effect occurred after the corresponding isothermal annealing. The condition of the samples in the holder after the cyclic annealing is shown in Fig. 7. Several rather big fragments of destroyed samples were found together with the fine beryllium dust. The size of one of such remnants from the isothermally annealed sample allowed its density to be measured and this result is

marked by an asterisk in Fig. 6. It seems that the swelling decrease in this case was caused by the formation of the open porosity.

The analysis of the optical microscopy images shows that the beryllium samples were fragmented into small blocks with a size distribution very close to the size distribution of grains in unannealed beryllium (see Figs. 8–10). The relative block area in the image plane was $21 \pm 2\%$ for the cyclic annealing case (Fig. 7) and $23 \pm 2\%$ for the isothermal one (Fig. 8).

The samples irradiated with a neutron fluence of $9 \times 10^{21} \text{ cm}^{-2}$ were solid after cyclic annealing at a maximum cycle temperature (700°C) without exposure and after the corresponding quasi-steady-state annealing. The results of the density measurement for these samples are given in Fig. 11.

The shape of samples irradiated with a neutron fluence of $9 \times 10^{21} \text{ cm}^{-2}$ before and after isothermal annealing at 800°C during 96 400 s is given in Fig. 12. The sample swelling after annealing calculated from the linear size change was about 20%, this value coincides rather well with the results of [5].

It is worth to mention that the samples increased in weight under annealing at 600°C, 700°C and 800°C due to oxidation of beryllium. The weight increase did not exceed $0.15 \pm 0.05 \text{ mg cm}^{-2}$ at 600°C and 700°C and about 90 mg cm^{-2} at 800°C. There was no correlation between the neutron fluence and the weight increase.

4. Discussion

A cyclic thermal loading of brittle materials with high anisotropy can lead to intergranular cracking at high enough heating/cooling rates [6,7]. The neutron irradiation causes an additional embrittlement of beryllium and, moreover, accumulation of a significant

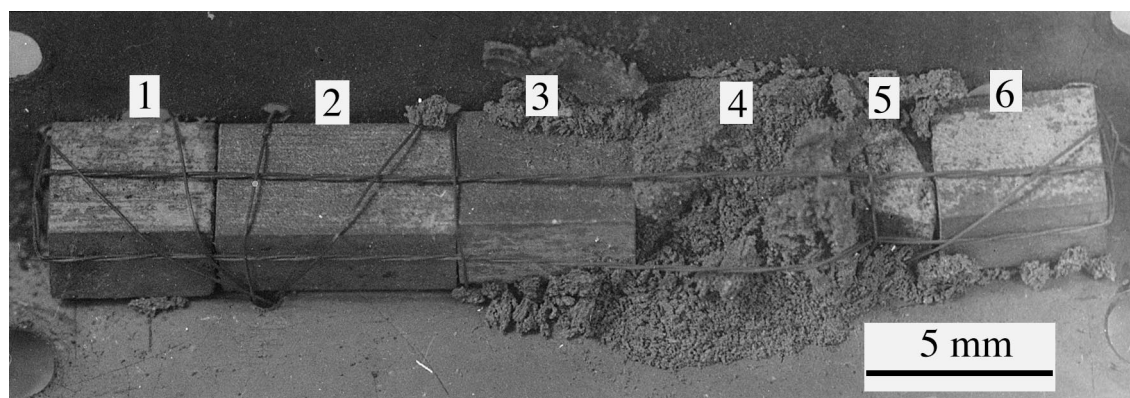


Fig. 7. Beryllium samples on the holder after 110 annealing cycles with exposure at the maximum cycle temperature (1 – unirradiated, 0.8 wt.% oxygen, 2 – neutron fluence $5 \times 10^{19} \text{ cm}^{-2}$, 3 – neutron fluence $3 \times 10^{21} \text{ cm}^{-2}$, 4 – neutron fluence $9 \times 10^{21} \text{ cm}^{-2}$, 5 – neutron fluence $1 \times 10^{21} \text{ cm}^{-2}$, 6 – unirradiated, 1.8 wt.% oxygen).

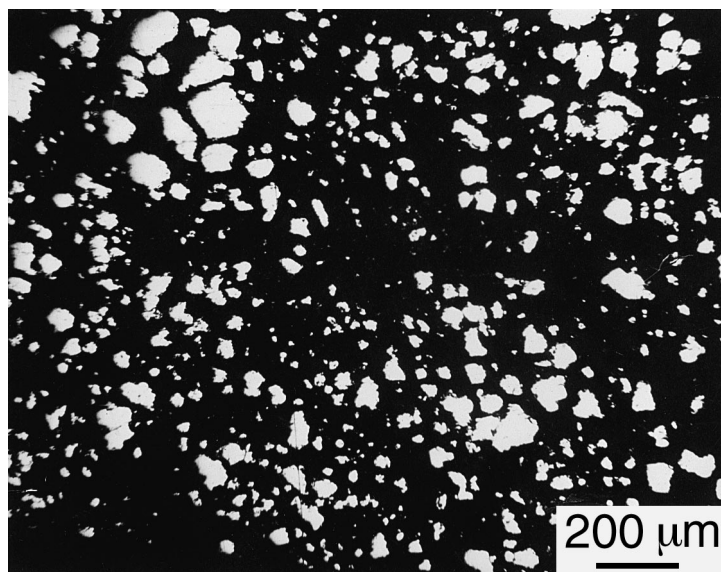


Fig. 8. Structure of the neutron-irradiated beryllium sample fragment (neutron fluence $9 \times 10^{21} \text{ cm}^{-2}$) after 110 annealing cycles at 700°C with exposure at the maximum cycle temperature. The image plane is perpendicular to the pressing axis.

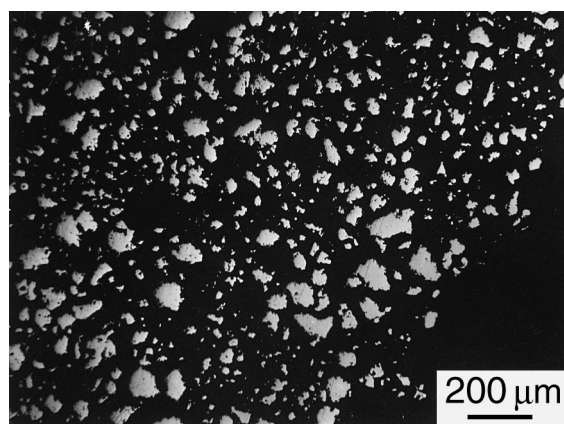


Fig. 9. Structure of the neutron-irradiated beryllium fragment (neutron fluence $9 \times 10^{21} \text{ cm}^{-2}$) after 96 400 s annealing at 700°C . The image plane is perpendicular to the pressing axis.

amount of gases. In spite of these circumstances, in accordance with the obtained results, there are no significant differences in the swelling values for the different annealing regimes. At the first glance a small cycling effect appears after 100 cycles without exposure at the maximum cycle temperature but there are not enough experimental data for the firm judgment of the presence of this effect and its value.

A close relative size distribution of grains in unannealed beryllium to blocks in the fragmented sample after 110 cycles at 700°C annealing with exposure at the maximum cycle temperature is evidence of the inter-

granular beryllium cracking and fragmentation. The reason for such a fragmentation after a long-time annealing of irradiated beryllium is probably internal stress-driven by the gaseous swelling [9]. These stresses achieve a maximum at the grain boundaries due to high beryllium anisotropy and preferential intergranular gas bubble formation [5,9]. These facts can lead to intergranular cracking up to full fragmentation as was described above.

The main plastic deformation mechanism for beryllium at low temperatures is the dislocation sliding, but at temperatures above T_{cr} (usually $T_{cr} > 600^\circ\text{C}$) the plastic deformation is mainly the result of the diffusion processes [10]. After neutron irradiation the dislocation mobility decreases because of the dislocation interaction with radiation defects such as point defects, helium and tritium atoms and their complexes. From these findings follows that diffusion processes are the prevalent mechanism of plastic deformation and stress relaxation in neutron-irradiated beryllium but its activation takes place only at high enough temperatures. So, the integrity of the beryllium sample with the maximum neutron fluence after long-time annealing at 800°C can be explained in contrast with the sample fragmentation at 700°C as the result of stress relaxation driven by the diffusion processes. There is an additional important factor explaining the absence of beryllium fragmentation at the annealing temperature of 800°C . This is a previously observed effect of the tritium burst release at about 750°C [5]. Such phenomena can lead to a beryllium deterioration at the annealing temperature of 800°C , i.e. at this temperature the most part of tritium has already left

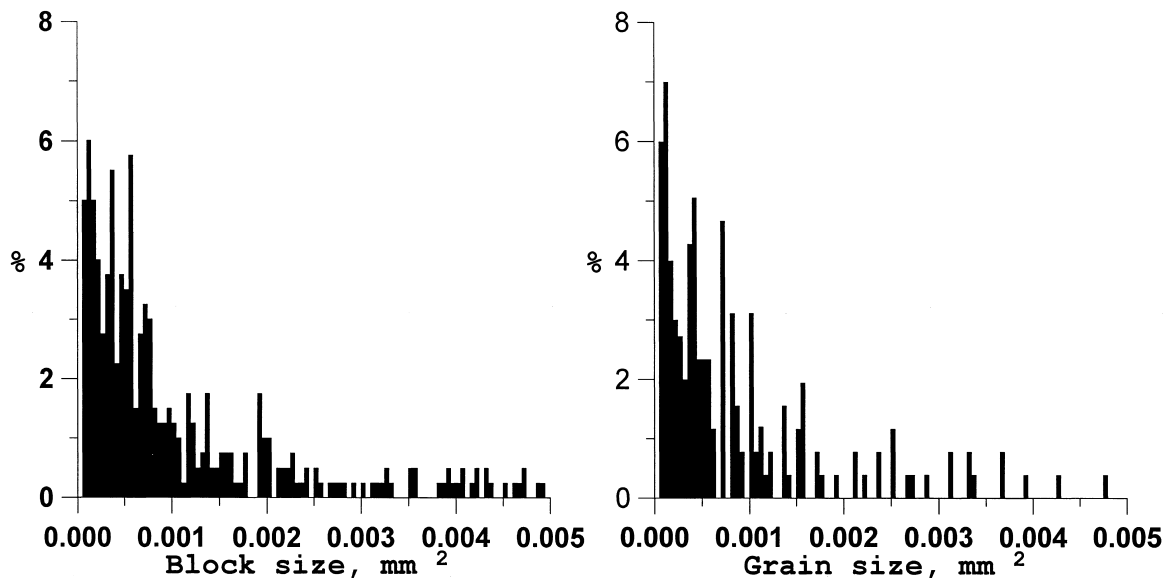


Fig. 10. Relative size distribution of grains in unannealed beryllium and blocks in the fragmented sample after 110 cycles of annealing at 700°C with exposure at the maximum cycle temperature.

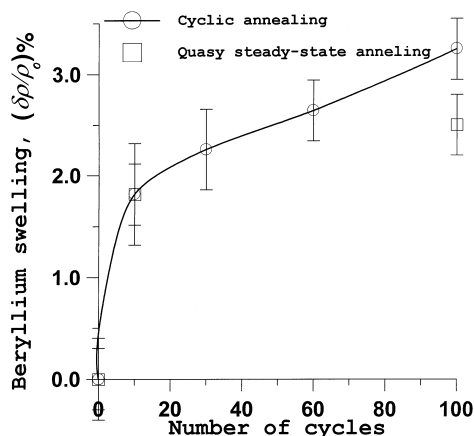


Fig. 11. Neutron-irradiated beryllium swelling dependence on the annealing duration in cyclic (without exposure at maximum cycle temperature) and quasi-steady-state regimes (maximum cycle temperature 700°C, neutron fluence $9 \times 10^{21} \text{ cm}^{-2}$). ρ_0 – beryllium density before annealing.

beryllium and cannot contribute to the grain boundary cracks and intergranular bubble growth. Simultaneously at this temperature the helium mobility is low and swelling due to helium diffusion is low too as evidenced by the previous results of the beryllium swelling investigation and hot vacuum gas extraction at linear heating [5,8].

From the investigations follows that annealings of neutron-irradiated beryllium at the cyclic temperature

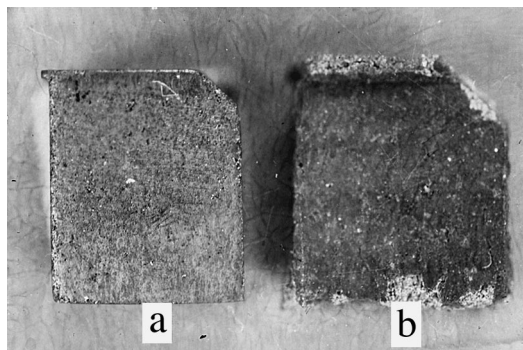


Fig. 12. Irradiated beryllium samples with neutron fluence $9 \times 10^{21} \text{ cm}^{-2}$ before (a) and after annealing at 800°C during 96 400 s (b).

change from 150°C up to 700°C at heating/cooling rates up to 10°C s^{-1} after 10–110 cycles have not shown significant differences in comparison with the isothermal or quasi-steady-state annealings.

It should be noted that under neutron irradiation at elevated temperatures the swelling value is significantly lower than after post-irradiation annealing [11], and similar beryllium cracking and fragmentation are not to be expected under the ITER conditions.

From these results it follows that under cyclic temperature change in the above described limits the main factors affecting the beryllium properties and structure are the maximum temperature and the exposure time at this temperature.

5. Conclusion

The cyclic thermal loading effect was negligible at the investigated heating/cooling rates (up to $10^{\circ}\text{C s}^{-1}$) and the number of cycles (up to 110). The main factors causing a property degradation of neutron-irradiated beryllium under these experimental conditions are the neutron fluence, the annealing temperature and the duration.

Annealing of the low-temperature neutron-irradiated beryllium can lead to beryllium fragmentation and formation of considerable amounts of beryllium dust. The main reasons of such fragmentation are the beryllium swelling causing the internal stresses at the grain boundaries and tritium migration to the grain boundaries. The absence of the beryllium fragmentation after annealing at 800°C can be explained by stress relaxation driven by diffusion processes and by the tritium release at elevated temperatures.

References

- [1] Technical basis for the ITER final design report, cost review and safety analysis (FDR), draft, San Diego ITER JWS, December, 1997.
- [2] ITER non-site specific safety report (NSSR-2), vol. 3, October, 1997.
- [3] G. Saji, private communication.
- [4] G.A. Sernyaev, M.V. Chernetsov, Yu.S. Strebkov, V.R. Barabash, Thermal cycling and initial density influence to the beryllium swelling, in: 3rd International Conference on Irradiation Influence to the Fusion Reactor Materials, September 1994, St-Peterburg, Russia.
- [5] D.V. Andreev, V.N. Bespalov, A.Y. Biryukov, B.A. Gurovich, P.A. Platonov, *J. Nucl. Mater.* 233–237 (1996) 880.
- [6] R.D. Watson, D.L. Youchison, D.E. Dombrowski, R.N. Guiniatouline, I.B. Kupriynov, *Fusion Eng. Design* 37 (1997) 553.
- [7] L.S. Youchinson, *Fusion Tech.* 29 (1996) 599.
- [8] D.V. Andreev, A.Yu. Biryukov, L.S. Danelyan, N.G. Elistratov, V.M. Gureev, M.I. Guseva, B.N. Kolbasov, Yu.Yu. Kurochkin, V.N. Nevzorov, O.V. Stativkina, A.M. Zimin, *Fusion Eng. Design* 39 & 40 (1998) 465.
- [9] V.P. Goltsev, G.A. Serniaev, Z.I. Chechetkina, *Radatsionnoe Materialovedenie Berillia*, Nauka i Tekhnika, Minsk, 1977, in Russian.
- [10] I.I. Papirov, G.F. Tikhinskii, *Plasticheskaia Deformatsia Beryllia*, Moscow, Atomizdat, 1973, in Russian.
- [11] D.S. Gelles, G.A. Sernyaev, M. Dalle Donne, H. Kawamura, *J. Nucl. Mater.* 212–215 (1994) 29.